Numerical Approximation of Elliptic Partial Differential Equations on soil-tool interaction problems using advanced nonlinear finite element approach

R.Jafari

***Abstract*-** The aim of this paper is to investigate finite element methods for the solution of the Sokolovski elliptic partial differential equation. The problem of solving such equations without triangulating surfaces is of increasing importance in various applications, and their discretization has recently been investigated in the framework of finite difference methods. For the two most frequently used implicit representations of surfaces, namely *level set methods* and *phase-field methods*, we discuss the construction of finite element schemes, the solution of the arising discretized problems, and provide error estimates. The variation of reacting force was plot under different solution methods and different input data. Results showed that the level set method outputs have less error than the phase- field method. Also the soil cohesion and mesh density have significant effect on the soil cutting forces.

***Keywords*-** level set method; phase-field method; Sensitivity Analysis; Soil–blade interaction simulation; finite element method

I. Introduction

The solution of partial differential equations on curves and surfaces has received growing interest in the last years due to a variety of applications in computer graphics [3, 4], materials science, and inverse problems. In many applications, elliptic or parabolic partial differential equations have to be solved on varying geometries, which means that after time-discretization a large number of elliptic problems remain to be solved numerically on different curves or surfaces. The standard approach to discretize these elliptic problems are finite element methods on curve or surface triangulations, which can cause a tremendous computational effort for varying geometries, since the triangulation has to be recomputed for each change in the geometry. Moreover, the approximation properties of such triangulations are not yet well understood except for simple geometries, and it is not clear how higher order geometric characteristics such as curvatures are to be represented on the triangulation. The soil failure mechanism under tillage tools operation can be represented by Sokolovski partial differential equation. Some analytical methods have been introduced to solve the soil- tools interaction problem [5, 6, 7, and 11]. Finite element method as a numerical approximation method have used by some researchers to model the soil tools interaction problem [12, 13]. The aim of present study is to introduce the numerical solution for Sokolovski equation and comparison the output of solution under different solution methods.

The author is Ramin Jafari, Assistant Professor Department of Agricultural Machinery, College of Agriculture, Shiraz University, Shiraz, Iran; phone: +987116138370; fax: +987112286104; e-mail: Rjafari@shirazu.ac.ir and Raminjafari1974@ yahoo.com.

II. Materials and Methods

In order to avoid surface triangulations, it seems reasonable to consider Eulerian methods based on implicit surface representations, which were used with great success in the construction of computational schemes for evolving curves and surfaces. By now the two standard Eulerian approaches for evolving surfaces are *level set methods* [8, 9] and *phase-field methods* [1, 2]. Level set methods are based on an extension of the equation on the surface to all level sets of an implicit representation function, ideally the signed distance function. Phase-field methods approximate the equation by a parameter-dependent reaction-diffusion equation, whose solution is an approximation of a rescaled signed distance function.

Eulerian schemes based on a level set representation of the surface have been proposed recently by Bertalmio et. al. The starting point of their analysis is an implicit representation of the surface, i.e., as the zero level set of a continuous function

$\varphi : R^d \rightarrow R$

$\Sigma = \{x \in R^d : \varphi(x) = 0\}$

The basic idea of the approach in is to rewrite the derivatives with respect to surface variables as projections of derivatives in Rd (with projection operators defined in terms of the level set function), and to extend the equations to a set D of positive Lebesgue measure in Rn. In particular, the surface gradient can be written as:

$\nabla_S U = P \nabla U$

$$P = I - \frac{\nabla\varphi \otimes \nabla\varphi}{|\nabla\varphi|^2}$$

 Manuscript received April3, 2008; Revised August 12, 2008

Using extensions of the coefficients, one can then extend the partial differential equation to all level sets.

$$\Sigma^{\alpha} = \{x \in R^{d} : \varphi(x) = \alpha\}$$

For all |α| sufficiently small, and thus, to a neighborhood of Σ, the implicit dependence on Σ is then replaced by dependence on $\nabla\varphi$. The benefit of this extension is the fact that standard discretization methods can be used in a small domain *D*, and therefore no surface triangulations are needed. The numerical methods in [4] and subsequent work were developed for the solution of time-dependent parabolic and hyperbolic equations, using explicit time-stepping. Stationary elliptic equations such as e.g. the Laplace-Beltrami equation, which appear in many applications either of interest for themselves [10] or as a sub problem in some larger system of equations have not yet been investigated. Moreover, all the schemes developed so far were based on finite differences on parts of a regular grid, while finite element methods allowing much more flexibility with respect to the grid have not yet been investigated in this respect. Phase-field methods for equations on surfaces have not yet been investigated in detail; such approaches are so far only considered as sub problems in the second-order splitting of fourth- order equations, with few rigorous arguments as the phase-field parameter tends to zero. The fundamentals of a phase-field representation are a phase-field function ψ, asymptotically of the form

$$\psi(x) = P(\frac{d(x)}{\varepsilon}) + \varepsilon q(x) + O(\varepsilon^{2})$$

Where d denotes the signed distance function to Σ, $\varepsilon > 0$ is a small parameter, and p is a monotone function such that P (-∞) =-1 and P (+∞) =1. Prototypes for the function p are:

$$P(s) = \frac{1}{\pi}\arctan(\gamma s) \qquad P(s) = \frac{2}{1+\exp(-s)} - 1$$

The first order expansion satisfies q = 0 on Σ, $||q||_{\infty} = O(1)$, and $||\nabla q||_{\infty} = O(1)$. In this paper, we shall investigate Eulerian methods for linear elliptic equations of the form:

$$-div(\alpha\nabla_{s}u) + cu = f, \qquad \text{on } \Sigma$$

Where div*S* and ∇s denote the surface divergence and gradient, respectively.

Level set representation: For an implicit representation with level set function ϕ, we can follow the formal argumentation given in [4] and extend as:

$$-\frac{1}{\nabla\varphi} div(|\nabla\varphi|\alpha^{\wedge}(0.\varphi)P\nabla u^{\wedge}) + C^{\wedge}(0,\varphi)U^{\wedge} = f^{\wedge}(0,\varphi)$$

With α^, *c* ^, and *f* ^ being appropriate extensions of the coefficients *a*, *c*, and. In order to obtain a consistent extension, one needs that

$$\alpha^{\wedge}(x,0) = \alpha(x) \quad c^{\wedge}(x,0) = c(x) \quad f^{\wedge}(x,0) = f(x), \qquad \forall x \in \Sigma$$

Phase-field representation: For an implicit representation with a phase-field function ψ, an approximation is given by:

$$-div((1-\psi^{2})\alpha(0,\psi)\nabla u) + (1-\psi^{2})C(0,\psi)u = (1-\psi^{2})f(0,\psi)$$

With a, c, and f being appropriate extensions of the coefficients a, c, and f. Consistency of the extension corresponds to the condition

$$\alpha(x,0) = \alpha(x) \quad c(x,0) = c(x) \quad f(x,0) = f(x), \qquad \forall x \in \Sigma$$

The phase-field function is assumed to satisfy an expansion. For simplicity we shall assume below that a, c, and f are constant extensions of a, c, and f in normal direction, but analogous results can be derived (with more complicated computations) for other sufficiently regular extensions.

A. Finite element formulation

The Elastic-Plastic model describes an elastic, perfectly plastic relationship. Stresses are directly proportional to strain until the yield point is reached. Beyond the yield point, the stress-strain curve is perfectly horizontal. A function which describes the locus of the yield point is called the yield function. The yield function of the Drucker- Prager elastic perfectly plastic material model (F) can be expressed as follows [14]:

$$F = 3\beta\sigma_{m} + [\frac{1}{2}\{S\}^{T}[M]\{S\}]^{0.5}$$

Where:

σ_{m} = the mean or hydrostatic stress= $\frac{1}{3}(\sigma_{x} + \sigma_{y} + \sigma_{z})$

{S}= the deviatoric stress equation

β = material constant and is equal to $\beta = \frac{2Sin\varphi}{\sqrt{3}(3 - Sin\varphi)}$

The material yield parameter is defined as

$$\sigma_{y} = \frac{6cCos\varphi}{\sqrt{3}(3 - Sin\varphi)}$$

Where:

C and φ are the input soil cohesion value and angle of soil internal friction, respectively.

Soil plasticity is formulated using the theory of incremental plasticity. Once a material begins to yield, the incremental strain can be divided into elastic and plastic components.

$$\{d\varepsilon\} = \{d\varepsilon^{p}\} + \{d\varepsilon^{e}\}$$

Only elastic strain increments $d\varepsilon^{e}$ will cause stress changes. As a result, stress increments can be written as follows:

$$\{d\sigma\} = [C_{e}]\{d\varepsilon^{e}\} = [C_{e}](\{d\varepsilon\} - \{d\varepsilon^{p}\})$$

A yield function, F, is a function of normal and shear stress, so an incremental change in the yield function is given by:

$$dF = \frac{\partial F}{\partial\sigma_{x}}d\sigma_{x} + \frac{\partial F}{\partial\sigma_{y}}d\sigma_{y} + \frac{\partial F}{\partial\sigma_{z}}d\sigma_{z} + \frac{\partial F}{\partial\tau_{xy}}d\tau_{xy} = \{\frac{\partial F}{\partial\sigma}\}\{d\sigma\}$$

The theory of incremental plasticity dictates dF will be equal to zero when the stress state is on the yield surface. This condition is termed the natural loading condition, and can be written mathematically as:

$$dF = \{\frac{\partial F}{\partial\sigma}\}\{d\sigma\} = 0$$

The plastic strain is postulated to be:

$$\{d\varepsilon_{p}\} = \lambda\{\frac{\partial G}{\partial\sigma}\}$$

Where, G and λ are plastic potential function and plastic scaling factors, respectively.

Finally the incremental stress corresponding to a given incremental strain is obtained as follows:

$$\{d\sigma\} = ([C_e] - [C_p])\{d\varepsilon\}$$

B. Finite element mesh and boundary conditions

The soil media is modeled as 100×70×80 Cm, (length× width× height) cube of solid material (fig.1). At the places that the cutting blade contacts with soil, the shape of the blade is carved into the soil. For both soil and blade, element solid 45 is used. Solid 45 is a brick element with 8 nodes and 3 degrees of freedom at each node (Ux, Uy, Uz).

Due to the symmetric geometry of the model, one half of the model was simulated but all the results consider the complete model. Two failure surfaces were predefined, one along the horizontal plane in front of the blade-cutting tip and the other along a vertical plane at a distance of 100mm from the symmetric plane and of height 200mm, i.e. along the blade vertical boundary, as shown in Fig. 1. The concept of master and slave contact (contact and target element) was used to simulate the interface between the cutting blade and the soil; and soil itself along the predefined failure surfaces. Relative motion was allowed with friction along the soil–tool and soil–soil interface surfaces. The model was meshed in a manner that increased the mesh density near the blade and the predefined failure surfaces.

The boundary conditions of the model are (Fig. 1)

1. Bottom base nodes, at Y=0, are fully constrained.
2. Nodes on vertical boundaries parallel to the Y–Z plane, at X=0 and X=1000mm, are constrained in the horizontal direction along X axis.
3. Nodes on vertical boundaries are constrained in the lateral direction along z axis.
4. The blade is constrained in the vertical direction and from any rotation but it is free to move in the horizontal direction along X axis.

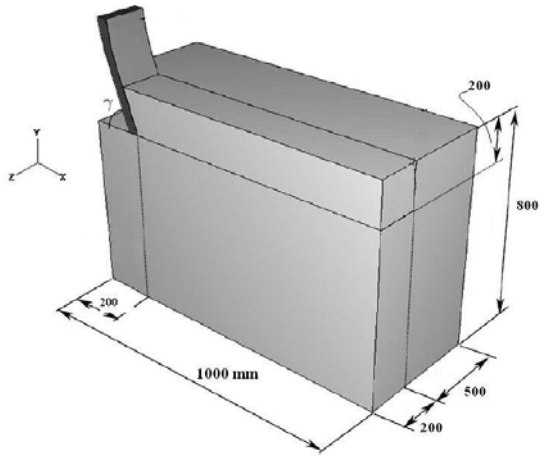

Fig.1. Soil–tool interface model dimensions.

The effects of variables on the soil reaction forces were investigated. Variables are:

Solution methods at two methods (level set and Phase-field methods)

Soil cohesion in three levels (10, 25 and 40 kpa)

Mesh density in two levels (fine and coarse meshing)

III. RESULTS AND DISCUSSION

The finite element results extracted from sensitivity analysis were calculated. The sensitivity of the reacting forces with respect to the input data was measured. The rate of increase of draught force is relatively high at low displacement, and levels out as displacement further increases. The reason for this process is that the plastic strain in each element occurs under very low displacement. In the next step of tool motion, the yielded elements transfer forces to their adjacent element and their force tends to become constant. The trend of reaction force variation with respect to the tillage tool displacement in different solution methods and different level of soil cohesion and mesh density was calculated and compared. The results in summery are:

A. The effect of solution method

The resulting errors for different discretization levels are given in figures 2 and 3. One observes that the magnitude of the errors is very low in the level set case. In order to compare the effect of the different extensions, we plot the solutions obtained with the level set and the phase-field representation in Figures 2 and 3. Comparison of the result extracted from experimental tests and two solution methods showed that the level set method data are closer to experimental one.

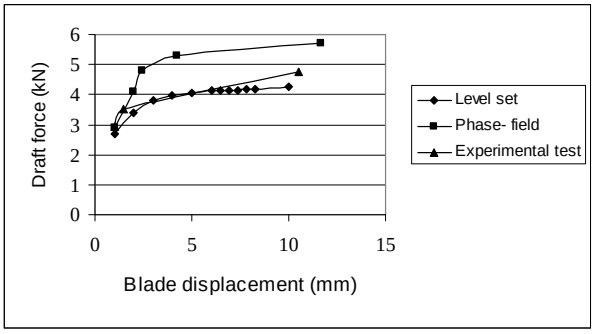

Figure.2. Variation of horizontal draft force according to the solution methods.

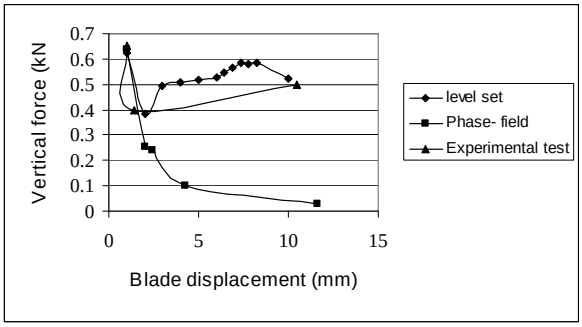

Figure.3. Variation of vertical reaction force according to the solution methods.

B. The effect of soil cohesion

The variation of draft force with respect to tool displacement at three level of soil cohesion showed that any increase in soil cohesion cause an increase in the steady state level of horizontal draft force. The maximum horizontal draft force has seen in the maximum level of soil cohesion. The direct relation between the soil cohesion and soil stiffness might be the main reason of such difference (Fig.4). The trend of horizontal draft force variation with respect to tillage tool displacement is similar to the hyperbolic stress- strain curve. In the loosen soils the draft force will be reached to the maximum level sooner than that of in the soil with higher cohesion. This is the main reason that the finite element analyses were diverged in the loosen soil sooner than the hard soil, because the soil elements will reach to the maximum allowable plastic strain in a lower displacement.

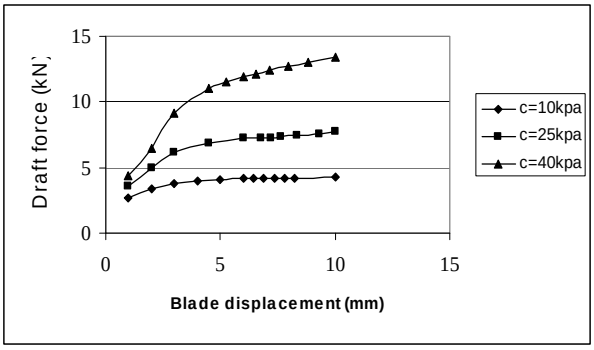

Figure.4. Variation of horizontal draft force according to the tool displacement at various level of soil cohesion.

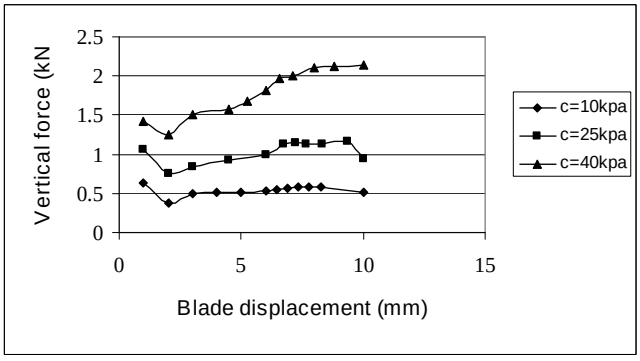

Figure.5. Variation of vertical reaction force according to the tool displacement at various level of soil cohesion.

The variation of vertical reacting force according to the tool displacement at three levels of soil cohesion showed that the force will level out after initial fluctuations (Fig.5). The trend of the variation of the vertical force is the same at different level of soil cohesion but the steady state vertical force level is higher in more cohesive soils than less cohesive soils. The calculated results showed that in the range of 15-40 kg/cm3 soil cohesion, the sensitivity of the variation of draft force and vertical force are 26.6 $\frac{kN}{kg/cm^2}$ and 0.05 $\frac{kN}{kg/cm^2}$ respectively.

C. The effect of mesh density

The effect of mesh density on the reliability of the 3D finite element model was investigated at two level of mesh density. The soil was meshed to 10 elements per width of cutting blade in fine meshing while in coarse meshing the width of blade was divided into 5 elements. Mesh density was found to have a very significant effect on the predicted results when using elastic-plastic material models to simulate soil–blade interface problem. To investigate the effect of the mesh density on the predicted finite element results of a 3D soil–blade interaction, a series of 3D finite element models was carried out for different various mesh densities and for 15mm of blade displacement. Predicted cutting forces acting on the blade in both draft and vertical directions were monitored during each finite element analysis and presented in Figs. 6 and 7, respectively, through 15mm of horizontal blade displacement. Fig. 9 represents the progress in draft cutting forces as the blade moves horizontally and Fig. 7 represents the progress in vertical cutting forces as the blade moves horizontally using various mesh densities. From these two figures it is noticeable that the mesh density has a very significant effect on the predicted forces in both draft and vertical directions in that as the mesh density increases the predicted forces decreases. For example, the reduction of the predicted forces can be in the order of 25% with slight increase in the mesh density. Results showed that to obtain a highly accurate quantitative analysis, a very dense mesh should be considered with an expected 2-day run time using a dual xenon 1 GHz processor PC with 500MB of memory.

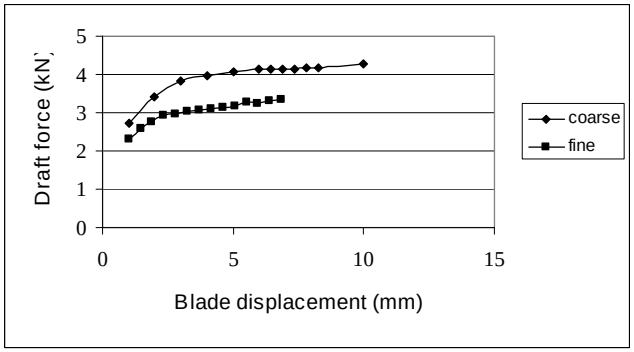

Figure.6. Variation of horizontal draft force according to the tool displacement at various level of mesh density.

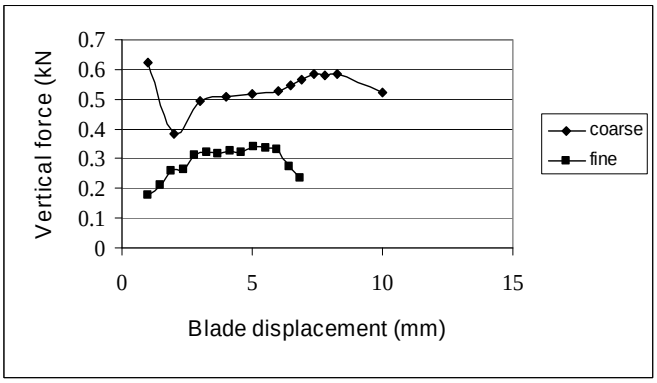

Figure.7. Variation of vertical force according to the tool displacement at various level of mesh density.

IV. Conclusion

The 3D finite element analyses have been carried to simulate soil–blade interaction and study the effect of blade soil properties and mesh density on predicted cutting forces in both draft and vertical directions. The so called elastic-plastic constitutive model was used to describe the behavior of the simulated soil in monotonic loading. The mesh density was found to have a significant effect on the predicted results. So only a qualitative study has been reported here. A series of models were analyzed concerning various solution methods, soil cohesion and mesh densities using 3D models. From the various 3D analyses carried out, some concluding remarks can be made as follows:

1. Comparison of the result extracted from experimental tests and two solution methods showed that the level set method data are closer to experimental one.
2. Soil cohesion has a significant effect on the cutting forces. The trend of variation of reacting forces according to blade displacement is the same at various levels of cohesion.
3. The mesh density has a significant effect on the predicted results in both draft and vertical directions in that as the mesh increases the predicted forces decreases.

V. References

[1] G.Barles, H.M.Soner, P.E.Souganidis, Front propagation and phase field theory, SIAM J. Control Optim. 31 (1993), 439-469.
[2] G.Caginalp, E.Socolovsky, Phase field computations of single-needle crystals, crystal growth, and motion by mean curvature, SIAM J. Sci. Comput. 15 (1994), 106-126.
[3] U.Diewald, T.Preusser, M.Rumpf, Anisotropic diffusion in vector field visualization on Euclidean surfaces, IEEE Trans. Vis. Comp. Graph. 6(2000), 139-149.
[4] J.Dorsey, P.Hanrahan, Digital materials and virtual weatherings, Scient. Amer. 282:2 (2000), 46-53.
[5] D. R. P. HETI'IARATCHI and A. R. REECE, Symmetrical three-dimensional soil failure. J. agric. Eng Res. 4 (1967), 45-67.
[6] R. J. GODWlN and G. SPOOR, Soil failure with narrow tines. J. agric. Eng Res. 22 (4), (1977), 213-228.
[7] E. McKYES and O. S. ALI, The cutting of soil by narrow blades, d. Terramechanics 14 (2), (1977), 43-58.
[8] S.J.Osher, R.P.Fedkiw, The Level Set Method and Dynamic Implicit Surfaces (Springer, New York, 2002).
[9] S.J.Osher, J.A.Sethian, Fronts propagating with curvature-dependent speed: algorithms based on Hamilton-Jacobi formulations, J. Comp. Phys. 79 (1988), 12{49.
[10] G.Turk, Generating textures on arbitrary surfaces using reaction-diffusion, Computer Graphics 25 (1991), 289-298.
[11] J. V. PERUMPRAL, C. S. GRISSO and C. S. DESAI, A soil-tool model based on limit equilibrium analysis. Trans. Am. Soc. agric. Eng. 26 (4), (1983), 991-995.
[12] R. N. YONG and A. W. HANNA, Finite element analysis of plane soil cutting. J. Terramechanics 14 (3), (1977), 103-125.
[13] R. L. KONDNER and J. S. ZELASKO, A hyperbolic stress-strain response: cohesive soil. J. Soil Mech. Foundation Div., ASCE 89 (SM1), (1963), 115-143.
[14] Ansys documentation, Release 8.1.